

## STRUCTURE CHARACTERIZATION OF CALCIUM DEFICIENT ELEMENT-SUBSTITUTED HYDROXYAPATITE WITH CONSTANT DOPANT RATIO OF DIFFERENT ELEMENTS

H. Al-Sabbagh<sup>1</sup> W. K. Salih<sup>1,3</sup> K. M. Thajeel<sup>1</sup> D. L. Goloshchapov<sup>2</sup>  
 Researcher Researcher Researcher Professor

<sup>1</sup> Materials research directorate, Ministry of Science & Technology, Baghdad, Iraq.

<sup>2</sup> Voronezh State University, Voronezh, Russia

<sup>3</sup> Corresponding author : email: [alwathiq316@yahoo.com](mailto:alwathiq316@yahoo.com), Mobile: 07903336291

### ABSTRACT

The element-substituted calcium Deficient hydroxyapatite samples were synthesized using liquid-phase precipitation method. Different element ions ( $Mg^{+2}$ ,  $Zn^{+2}$ , and  $Cu^{+2}$ ) were added at constant ratio (5% wt.). The phase composition of the element-substituted calcium hydroxyapatite samples was investigated by using X-ray diffraction. A comparison with known characteristics of the synthetic ion-substituted forms of hydroxyapatite was conducted. It was determined, that the investigated materials are single-phase solid solutions of the element-substituted hydroxyapatite. By the methods of IR spectroscopy and Raman scattering (RS) it was discovered the dependence of incorporation of the carbonate anion that occupies a positions of phosphorus-oxygen groups in the hydroxyapatite structure as a result of embedding element ions ( $Zn^{+2}$ ,  $Cu^{+2}$ ,  $Mg^{+2}$ ) in the crystal lattice. Besides, It was determined, that the ratio of the intensities for the  $CO_3$  group mode to the  $PO_4$  groups mode depended on the nature of the element atom, which replace the calcium in the lattice of HAP, and reduced by substituting the calcium atoms by the atoms of Zn, Cu, and Mg from 0.15 to 0.06. Modeling of the vibration modes of Raman spectroscopy showed that incorporation of carbon atoms to the hydroxyapatite structure correlate with the Zn, Cu and Mg atomic radius, charge, and activity

**Keywords:** Hydroxyapatite, XRD, FTIR, Raman, Dopant element, Mg, Cu, Zn

الصباغ وآخرون

مجلة العلوم الزراعية العراقية -2020: 51(5): 1420-1427

التشخيص البنيوي لماده الهيدروكسي ابيتايت منقوص الكالسيوم معوض بنسبه ثابتة من مختلف المعادن

هيثم الصباغ<sup>1</sup> واثق كريم صالح<sup>1</sup> خالد مهدي ثجيل<sup>1</sup> ديمتري كولوشجابوف<sup>2</sup>

باحث باحث باحث باحث

<sup>1</sup> دائرة بحوث المواد /وزارة العلوم والتكنولوجيا / بغداد / العراق

<sup>2</sup> جامعة فارونيش / فارونيش / جمهورية روسيا الاتحادية

المستخلص

تم تصنيع نماذج من مادة الهيدروكسي ابيتايت المنقوص الكالسيوم المعوض بمختلف العناصر بطريقة ترسيب الطور السائل. تمت اضافة أيونات العناصر مثل النحاس والرصاص والزنك وبنسبة اضافته ثابتة هي 5% للهيدروكسي ابيتايت. تمت عملية فحص التركيب والطور بواسطة استخدام منظومة حيود الأشعة السينية للنماذج المحضرة. بينما دراسة الخواص المجهرية جرت باستخدام منظومتي مطياف الأشعة تحت الحمراء وجهاز رامان. لقد بينت نتائج تحليل الطور والتركيب بان الطور المتكون لجميع النماذج هو طور احادي. اما نتاج الفحوص المجهرية فبينت اعتماد وجود مجموع الكاربونات السالب في مواقع ايونات مجموع الفوسفات على وجود المعادن المضافة في البنية البلورية للهيدروكسي ابيتايت. إضافة لذلك، فقد وجد ان نسبة مجموع الكاربونات السالبة الى مجموع الفوسفات الموجبة تعتمد على طبيعة ذرات العنصر المعوض للكالسيوم في البنية البلورية للهيدروكسي ابيتايت. ان نموذج الاشكال الاهتزازية المتحري عنها باستخدام جهاز رامان اظهرت ان هناك ترابطا بين وجود مجموع الكاربونات مع اقطار ذرات العناصر المعوضة للكالسيوم الزنك والنحاس والمغنيسيوم وشحنتها وفعاليتها.

الكلمات المفتاحية: هيدروكسي ابيتايت، حيود الأشعة السينية، الأشعة تحت الحمراء، رامان، معادن مشوية، مغنيسيوم، نحاس، زنك

\*Received:11/8/2019, Accepted:21/11/2019

## INTRODUCTION

The analysis of the solid tissues of the human skeleton and the detection in vivo of defects, pathogenic formations, as well as degradation of biomaterials are difficult and time-consuming task. At the present stage of the development of the dental analysis methods, the biological samples of calcium hydroxyapatite (HAP) - the basic mineral component of a bone tissue of the human skeleton is carried out with using of infrared spectroscopy and Raman scattering. These methods, side by side with X-ray diffraction, allow the identifying of the change in the phase composition, the discovering of the inclusion of external complexes in the structure of the substance and registering differences in the molecular bonds of biological compounds. Despite a large number of scientific papers, devoted to this subject, the problem of interpretation of the data obtained from biomaterials is the actual ones. This fact is explained by the presence of a large number of various kinds of metals and the presence of all the objects under consideration in the nano-form of the biomaterials of hard tissues, which significantly complicates the described problem. On the other hand, in the literature works on the synthesis of nanomaterials based on hydroxyapatite, it's well known, which include impurity of atoms and groups in different concentrations. By the considerations and the properties of these compounds - analogs of the solid tissues of the human skeleton, as well as the expansion of data on their spectroscopic characteristics will help to give us a solution and a rapid assessment for the problem of the presence of possible pathologies, for example, detecting the growing process of the enamel caries. By considering the problems of implanting the element ions into the crystal lattice of HAP for modeling biological objects, it should be noted, that biogenic hydroxyapatite includes various ( $\text{Na}^{+1}$ ,  $\text{Mg}^{+2}$ ,  $\text{Sr}^{+2}$ ,  $\text{K}^{+1}$ ,  $\text{Fe}^{+2}$ ,  $\text{Zn}^{+2}$ ,  $\text{Cu}^{+2}$ ,  $\text{Ba}^{+2}$ ,  $\text{F}^{-3}$ ,  $\text{Cl}^{-1}$ ,  $\text{C}^{+4}$ ,  $\text{S}^{-2}$ ), are participating in the processes of osteogenesis. Wherein, researchers pay special attention to the processes of accelerating or slowing the formation of new bone tissue, as well as antibacterial effects, this is due to the ions insertion into the structure of synthetic

materials similar to the series indicated for the biogenic HAP. In the literatures of synthesis HAP, the structure characteristics and the possibility of replacing atoms of Calcium with atoms of different elements, led to the highlighting of such ions as  $\text{Zn}^{+2}$ ,  $\text{Cu}^{+2}$ ,  $\text{Mg}^{+2}$  due to their influence on all processes of osteosynthesis. Despite the positive results on the use of pure hydroxyapatite  $\text{Ca}_{10}(\text{PO}_4)_6(\text{OH})_2$  in surgery and dentistry, researchers are looking for ways to improve its osteoconductive characteristics. One of these ways is to implant ions of different elements into the lattice of HAP, which is contained in mineralized tissues (5, 8, 18). It is known, that the behavior of the synthetic material in the body environment depends on the change in the structure of hydroxyapatite and the activity and properties of element ions that would be implanted because they affect on the behavior of the entire material in the body environment. The Existing data indicate a variety of physicochemical, thermal characteristics of the samples, determined by the type and degree of substitution of calcium atoms by other atoms (1, 6, 7, 17). During 2015, Friederichs and his team investigated the effect of ionic co-substitution in hydroxyapatite (HA). The Zinc, silicate co-substituted HA (ZnSiHA) remained phase pure after heating to  $1100^\circ\text{C}$  with Zn and Si amounts of 0.6 wt% and 12 wt %, respectively (10). In the work of Esfahani and his team in 2016, the structural and morphological analysis of Zn incorporated non-stoichiometric hydroxyapatite (nHAp) nano powder was done. The preparation method was the precipitation method (9). In 2016, Zilm and his team fabricated HA substituted by transition elements [ $\text{Mn}^{+2}$ ,  $\text{Fe}^{+2}$ ,  $\text{Co}^{+2}$ ]. They compared the theoretical results with experimental ones. They concluded that the results of three types were in good agreement with theoretical ones and HA doped by  $\text{Mn}^{+2}$  had the greatest effect on the magnetic properties (27). In 2017, Robles-Águil and his team synthesized Calcium Hydroxyapatite doped different elements using sol gel microwave assisted method. They concluded that elements ions did not affect on lattice volume of hydroxyapatite (23). In 2018, Negrila and his team prepared Zinc doped hydroxyapatite using sol gel

method and ultrasound characterization was done to specify the effect of Zinc on HA properties (19). In 2018, Phatai and his co-workers synthesized Cerium doped hydroxyapatite via sol gel preparation method with assisted ultrasonic technique (21). In 2019, Zhang and his team used Zinc and strontium as co-dopant for HA. They noticed that HA formed with low crystallinity and disorder lattice (26). Also in 2019, Ofudje and his workers could manufacture antibacterial and scaffold Zinc doped hydroxyapatite for medical applications via chemical coprecipitation technique (20). The structure of hydroxyapatite and its substituted forms: Hydroxyapatite (HAP)  $[Ca_{10}(PO_4)_6(OH)_2]$  is a major component of the inorganic part of bone, however its chemical composition is complicated in reality, non-stoichiometric and Calcium-deficient (Ca/P molar ratio < 1.67) due to vacancies, foreign cations and anions such as Sodium, Zinc, Magnesium, Iron and Carbonate ( $CO_3$ ), which are taken up from the surrounding body fluids during bone metabolism. The structure and the atoms configuration in HAP are clarified in Fig 1., which shows the hexagonal unit cell of hydroxyapatite HA occurs in a hexagonal crystal structure (space group P63/m) with 44 atoms per unit cell and lattice parameters  $a = b \neq c$  and  $\alpha = \beta = 90^\circ$ ,  $\gamma = 120^\circ$ . The unit cell and the local environment of Ca in pure HA are shown in Fig. 1. There are two distinct Ca sites where cation exchange may occur. The Ca(I) site is surrounded by nine Oxygen ions from the surrounding phosphate tetrahedron and forms a distinct Ca channel parallel to the c-axis. The Ca(II) site is surrounded by six oxygen ions from five phosphate groups and the hydroxyl ion. The Ca(II) ions form triangular bases staggered above and below by the OH ion. The OH ion similar to Ca(I), forms a distinct channel parallel to the c-axis. Based on the distance and the coordination number of oxygen and calcium, three Oxygen atoms are defined as O(1), O(2) and O(3). The oxygen in OH is defined as OH. Thus the formula for HA can also be written as  $Ca(I)_4Ca(II)_6(PO(I)O(II)O(III))_6(OH)_2$ . (8, 16, 27).

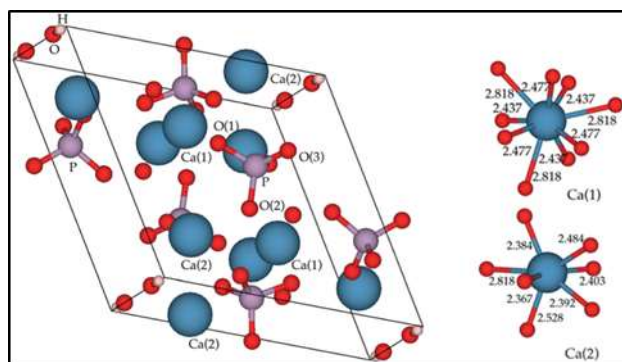


**Figure1. Location of Ca atoms,  $PO_4$  and OH groups in the unit cell of HAP (27).**

When considering the bone tissue of the human body and animals, the general formula for apatite biogenic samples can be much more complicated in view of the large number of impurity atoms included in the structure  $[Ca_{10-x-z}Me_z((HPO_4)_y(PO_4)_{1-y}(CO_3))_6(OH,F,Cl,CO_3)_x]$  (20). In the designated chemical formula of this compound, Calcium ions can link with metal ions (Me) : (Na, Mg, Sr, K, Fe, Zn, Cu, Ba, F, Cl, C, S) which perform an important function in the processes of osteogenesis. The incorporation of each of these ions into the crystal lattice of hydroxyapatite alters the properties of these materials (4) and may indicate the onset of the development of any process in bio-tissues. This fact is the reason for seeking the relationship between the structure and the manifested features in the spectra of various assay methods for nutrient materials (3, 25). The goal of this work is determination of the spectroscopic characteristics of the prepared samples of element - substituted hydroxyapatite from a change in the elemental composition and heat treatment.

## MATERIALS AND METHODS

**Chemicals and materials:** All chemicals which were used in this work are analytical grade manufacturing by Aldrich Company with 99% purity and using without purification. **L**

**Work procedure:** To obtain samples of Calcium hydroxyapatite and its substituted forms, a technique was used, which was mentioned in scheme described in (14, 24) in which the method of liquid-phase precipitation of HAP samples from a solution and inclusion of impurity atoms Zn, Cu and Mg was used. This technique was chosen to replace calcium atoms with element atoms, since theoretical and experimental results showed that

substitution in Calcium-deficient HAP has a high probability than in HAP without defects. As a basis for the method of obtaining samples was developed (2, 14). The steps of the synthesis process clarifies in Fig+ 2. In this work, samples of element-substituted forms of hydroxyapatite, in which the Calcium atoms are replaced by Zn , Cu , Mg atoms in a specific concentration of solid solutions to 5% of the each element. Unalloyed Calcium-deficient hydroxyapatite (CDHAP) was prepared by chemical precipitation from solution according to the following procedure. The preset amount of the 0.3 M  $(\text{NH}_4)_2\text{HPO}_4$  solution was gradually introduced into a solution of 0.5 M  $\text{Ca}(\text{NO}_3)_2 \cdot 4\text{H}_2\text{O}$ . Then, 25% ammonia  $\text{NH}_4(\text{OH})$  solution was added to the resulting slurry to obtain a pH value of 9.4. To obtain samples of Magnesium, Copper and Zinc-substituted HAP (MeHAP) , participating as in the reaction, 5% solutions of element salts  $\text{Cu}(\text{NO}_3)_2 \cdot 3\text{H}_2\text{O}$ ,  $\text{Zn}(\text{NO}_3)_2 \cdot 4\text{H}_2\text{O}$ ,  $\text{Mg}(\text{NO}_3)_2 \cdot 6\text{H}_2\text{O}$  were added . In all cases,

pH= 11 was achieved by adding a calculated amount of 25%  $\text{NH}_4(\text{OH})$  solution and mixing for 2h . Then, the curing process begins for 12h to reach to pH=9.4. After that, characterization tests are investigated.

#### Characterization Tests

**X-ray diffraction:** XRD-6000 SHIMADZU instrument using  $\text{Cu K}\alpha$ -1 radiation ( $\lambda = 1.5406 \text{ \AA}$ ) in the range of angles  $10^\circ - 90^\circ$  in  $0.1^\circ$  increments by using the International Center for Diffraction Data ( ICDD ) database – Japan.

**Infra-Red spectra:** VERTEX-70, Bruker. The transmission spectra were recorded with a resolution of  $0.01 \text{ cm}^{-1}$  with respect to the wave number and a background recording time of 32 sec in the range  $400\text{-}4000 \text{ cm}^{-1}$  – Germany.

**Raman spectroscopy:** The Senterra Raman Microscope Spectrometer Bruker, a step of  $0.5 \text{ cm}^{-1}$  in the range from 300 to 1200 – Germany.

**pH meter :** IPL-101 MULTIVER ,SPE SEMIKO company, Moscow, Russia.

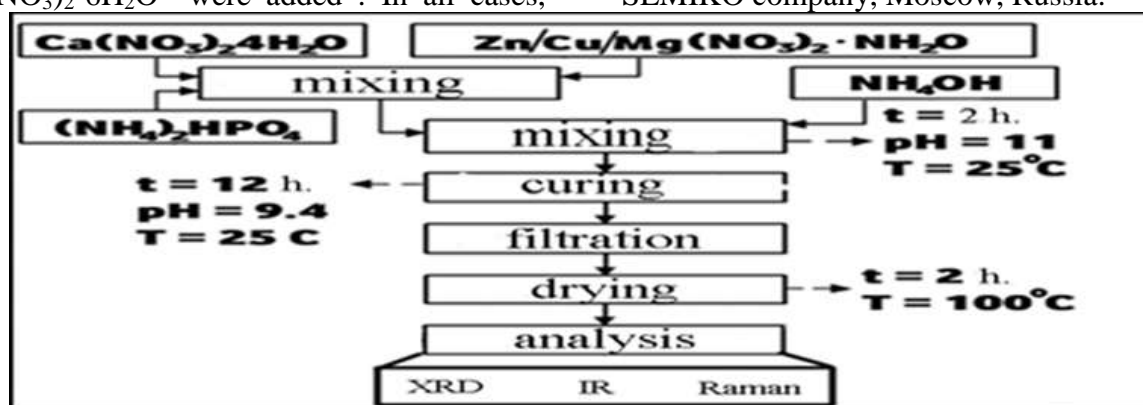


Figure 2. work procedure

## RESULTS AND DISCUSSION

### Composition characterization

**X-ray diffraction technique:** was used to determine the phase composition of the materials. X-ray phase analysis showed the formation of a single nano-crystalline phase of solid solutions of elements based on hydroxyapatite in all samples. Analysis of the diffractograms showed that prepared samples belong to Calcium hydroxyapatite. X-ray diffractometry for HAP investigations , which were thermally treated at  $100^\circ \text{ C}$  for samples with different elements with 5% concentration, have a formation of a single phase and represent Calcium deficient hydroxyapatite

$[(\text{Ca}_{10-x}\text{Zm}_{x})_y(\text{HPO}_4)_y(\text{PO}_4)_{1-y})_6(\text{OH})_2]$ , which remains stable for a long time. The XRD pattern of pure hydroxyapatite (without element substitution) is in agreement with ICDD database (JCPDS PDF# 9-432) as shown in Fig. 3 (curve 1) where the phase is belonged to Calcium hydroxyapatite. XRD pattern of element doped samples showed that phase did not change with doping process and the structure is same for all doped samples as shown in Fig. 3 (curve 2, 3, 4). It is noted the phase of HAP and Me-HAP is only hexagonal phase which is similar to most previous works (11, 22).

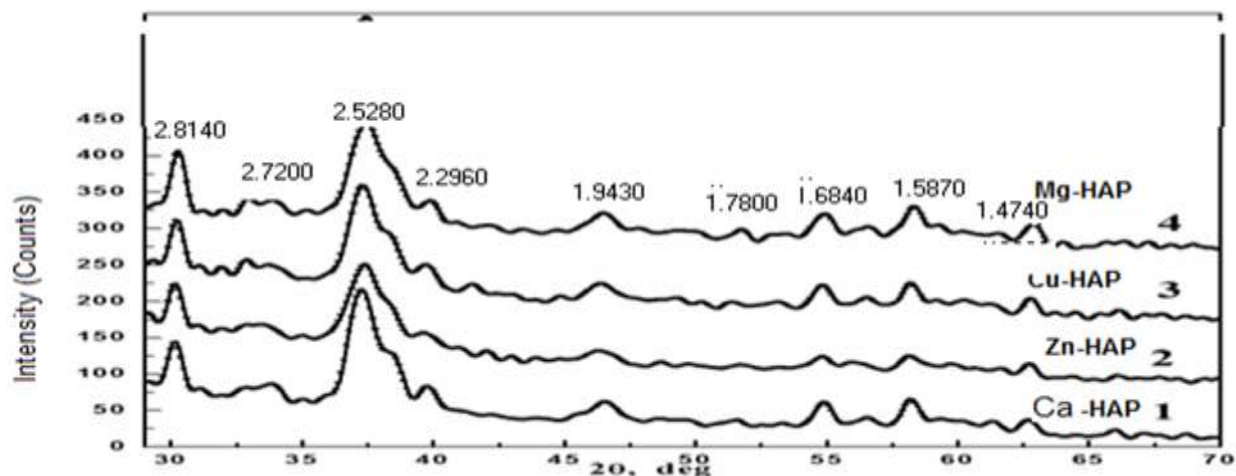


Figure 3. Patterns of XRD test

**FTIR characterization results:** Infrared Fourier spectroscopy (FTIR) was used to detect differences in the composition of the organic matrix of the samples. The study of IR spectra of the synthesized powders established the correspondence of the obtained materials - hydroxyapatite of Calcium with the inclusion of carbonyl anions  $\text{CO}_3^{2-}$ , especially noticeable in the uncontaminated HAP in the region of  $(1400 - 1450) \text{ cm}^{-1}$  instead of the  $\text{PO}_4$  groups (Figure 4, curve 1). While, the

carbonate concentration in element-doped samples reduced with varied concentrations according to element type Fig. 4 (curves 2, 3, 4). The regions  $(625, 960, \text{ and } 1130) \text{ cm}^{-1}$  are belonged to the  $\text{PO}_4$  group. Whereas,  $875 \text{ cm}^{-1}$  can be attributed to the  $\text{HPO}_4$  group which is classified as weaker group. Besides, the group of water molecules can be seen. The results are in compatible to those of Furko and his team (11).

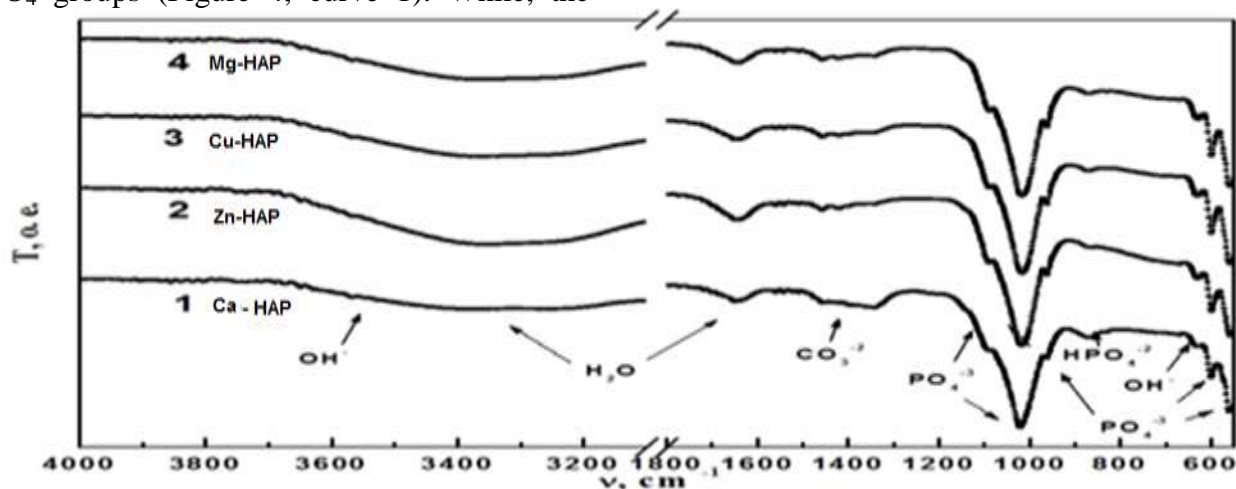


Figure 4. FTIR test results

**Raman Characterization:** Raman spectroscopy test was used to determine the presence of distortions in the hydroxyapatite lattice. The results confirmed the decrease in the inclusion of anion carbonate in structure of element-dopant Synthesized HAP samples as a result of the incorporation of Zn, Cu, Mg element ions into the crystal lattice of dopant HAP samples comparing with the carbonate ratio in Ca-HAP. Fig. 5 shows the Raman spectra, where the curves 1 - 4 relate, respectively, Ca-HAP, Zn-HAP, Cu-HAP, Mg-HAP respectively. As can be seen from

the Fig. 5, the spectra composition of the element-substituted samples remains unchanged and corresponds to hydroxyapatite (15). The modes at  $960.5 \text{ cm}^{-1}$  refer to the vibrations ( $\nu_1$ ) of the  $\text{PO}_4$  group, by  $1047 \text{ cm}^{-1}$  to the vibrations ( $\nu_3$ ) of the same group, in the  $590 \text{ cm}^{-1}$  region and the  $609 \text{ cm}^{-1}$  to the ( $\nu_4$ ) group  $\text{PO}_4$ , and  $431$  and  $447 \text{ cm}^{-1}$  to ( $\nu_2$ ) of the  $\text{PO}_4$  group. The mode which is appearing in the Raman spectra of all samples at  $1070 \text{ cm}^{-1}$  refers to the group of  $\text{CO}_3$ , which is introduced into the location of the  $\text{PO}_4$  group during the synthesis of the samples and

correlates with the data of IR spectroscopy. It is noted that the intensity of this mode with respect to the mode  $960.5\text{ cm}^{-1}$  ( $\nu_1$ ) of the  $\text{PO}_4$  group does not depend on the degree of substitution. The relative intensity of this mode with respect to the modes of the  $\text{PO}_4$  group depends on the nature of the substituting element to the Calcium atom in the HAP lattice, and is due to its activity. The expansion of the absorption bands of Raman spectra in

the region  $(1000-1100)\text{ cm}^{-1}$ , showed, that the relative intensity of the mode of the  $\text{CO}_3$  group to the mode of the  $\text{PO}_4$  group decreases with the replacement of the Calcium atoms by Zn, Cu and Mg atoms from 0.15 to 0.06 because the high tendency of Calcium ion to bond with Carbonate ion in comparing with other elements. So, the ratio of this group decreased when the Calcium was substituted with other element ion  $\text{Mg}^{+2}$ ,  $\text{Zn}^+$  and  $\text{Cu}^{+2}$ .

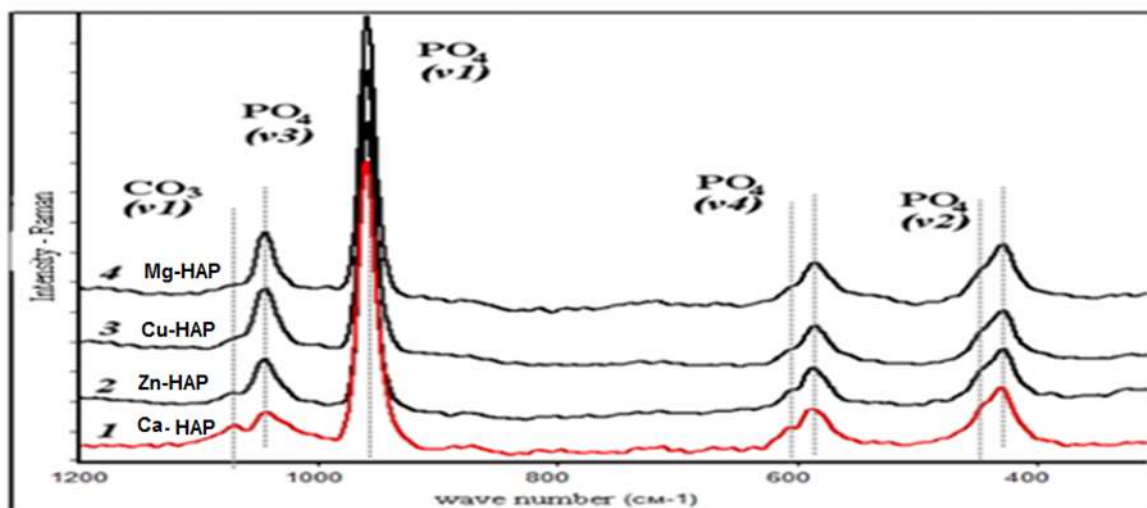


Figure 5. Ramman results

**Carbonate /Phosphate Ratio:** Since, that the Raman spectra show a different dependence on the type of cation being introduced in Fig. 6, one of the factors that possibly affects on the degree and the nature of the defects in the element-substituted Calcium hydroxyapatite is presented: the relative intensity of the  $\text{CO}_3/\text{PO}_4$  modes in HAP and Me-HAP together with the atomic radii of the cations introduced. The ratio between the intensity of the mode of the anion of carbonate to the intensity of the Phosphate group varies with the radius of the

element atom. As shown in the Fig. 6, for some of the atoms, is true. But it should be said, that this intensity ratio, shows that the presence of an anion of carbonate in the structure is determined, as well as chemical activity for each element atom, and the process of charge compensation with the growth and formation of HAP crystals and the atomic environment of each substituent ion (13).the lowest  $\text{CO}_3/\text{PO}_4$  is recorded for Mg element substituted Hydroxyapatite (Mg-Hap) in spite that radii of Mg atom is bigger than Zn, Cu.

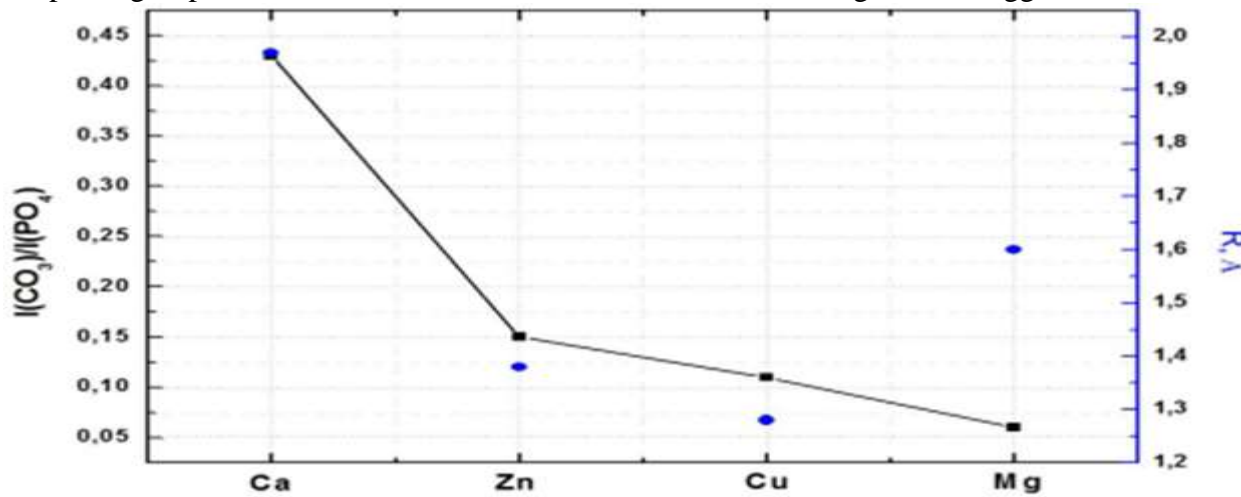


Figure 6.  $\text{PO}_4/\text{CO}_3$  ratio

**CONCLUSIONS**

X-ray phase analysis using the ICDD database showed the formation in all samples of a single nano-crystalline phase of solid solutions of elements based on hydroxyapatite. The study of the IR spectra of synthesized powders established the correspondence of the obtained materials - hydroxyapatite of Calcium with the inclusion of carbonyl anions  $\text{CO}_3^{2-}$  in the carbonate structure, especially noticeable in pure HAP in the region of  $(1400-1450) \text{ cm}^{-1}$ . The low-intensity modes detected in the region of  $820 \text{ cm}^{-1}$  and  $(1340-1380) \text{ cm}^{-1}$  belong to the group  $\text{NO}_3^{-1}$ , adsorbed on the surface of powders during the synthesis. The contribution of each of the substituent cations is detected by the effect on the mode position of the  $\text{PO}_4$  group, as evidenced by the shifts of the transmission bands in the IR spectra of all the samples. Investigation of Raman spectra confirmed a decrease in the inclusion of carbonate anions in the structure of HAP as a result of the incorporation of Zn, Cu, Mg element ions into the crystal lattice of HAP. Investigation of Raman spectra, in the revealed modes, characterizes hydroxyapatite ( $431, 447, 590, 609, 961, \text{ and } 1047) \text{ cm}^{-1}$  in all spectra of the samples. The mode appearing in the Raman spectra of all samples at  $1070 \text{ cm}^{-1}$  refers to the group  $\text{CO}_3$ , which during the synthesis of samples is introduced into the location of the  $\text{PO}_4$  group. The relative intensity of this mode with respect to the modes of the  $\text{PO}_4$  group depends on the nature of the element atom that substitutes the Calcium atom in the HAP lattice, and is due to its activity.

**CONFLICT OF INTERESTS**

The authors declare that they have no conflicts of interest.

**REFERENCES**

1. Al-Hadethi A.A. H., M. N. A. AL-Falahi and A.S. Nema, 2019, some cations movement in calcareous soil columns under effect of saline water mixed with humic acid, Iraqi Journal of Agricultural Sciences, 50(5):1313-1323
2. Al-Zubaidi A. A., 2014, Investigation of the physicochemical properties of element-substituted nano-crystalline calcium-deficient hydroxyapatite Ph.D. thesis, physical and

mathematical sciences department, Voronezh State University, Voronezh, Russia

3. Amaechi B. T., 2009, Emerging technologies for diagnosis of dental caries: The road so far, J. Appl. Phys., 105(10) : article ID: 102047
4. Bigi A., E. R. Foresti, Gregorini, A. A., Ripamonti, N. Roveri and J. S., Shah 1992, The role of magnesium on the structure of biological apatites, Calcif. Tissue. Int., 50(5):439–444
5. Boanini E, M. Gazzano and A., Bigi 2010, Ionic substitutions in calcium phosphates synthesized at low temperature. Acta Biomater, 6 (6): 1882–1894
6. Combes C., S. Cazalbou and C.Rey, 2016, Apatite Biominerals, Minerals., 6(2):.25 p
7. Domashevskaya E. P., A. A. Al-Zubaidi, D. L. Goloshchapov, N. A. Rumyantseva and P. V. Seredin, 2014, Structure and composition of the metal - substituted calcium - deficient hydroxyapatite, J Surf Invest-X-Ray, 8(6): 1128–1136
8. Eliaz N. and N. Metoki, 2017, Calcium Phosphate Bioceramics: A Review of Their History, Structure, Properties, Coating Technologies and Biomedical Applications, Materials, 10, 334; doi:10.3390/ma10040334
9. Esfahani H., E. Salahi, A. Tayebifard, M. R. Rahimipour, and M. Keyanpour-Rad, 2016, Structural and morphological analysis of zinc incorporated non-stoichiometric hydroxyapatite nano powders, Matéria (Rio J.), 11726: 569-576
10. Friederichs R. J., H. F. Chappel, Shepherd D. V. and S. M. Best, 2015, Synthesis, characterization and modelling of zinc and silicate co-substituted Hydroxyapatite, J. R. Soc. Interface, 12(10):article ID: 20150190
11. Furkoa M., V. Havasi, Z. Konya, A. Grunewald, R. Detsch, A. R. Boccaccini and et al., 2018, Development and characterization of multi-element doped hydroxyapatite bioceramic coatings on metallic implants for orthopedic applications, Bol Soc Esp Ceram V., 57(2):55-56
12. Gomes S, J-M. Nedelec, E. Jallo, D. Sheptyakov, and G. Renaudin, 2011, Unexpected mechanism of  $\text{Zn}^{+2}$  insertion in calcium phosphate bioceramics, Chem Mater. J., 23 (2):3072–3085

13. Gutowska I., Z. Machoy, and B Machaliński, 2005, The role of bivalent metals in hydroxyapatite structures as revealed by molecular modeling with the Hyper Chem software, *J. Biomed. Mater. Res. A.*, 75A (4): 788–793
14. Lima I. R., G. G. Alves, C. A. Soriano, A. P. Campanelli, T. H. Gasparoto, and E. S. Ramos, 2011, Understanding the impact of divalent cation substitution on hydroxyapatite: an in vitro multiparametric study on biocompatibility, *J. Biomed. Mater. Res. A.*, 98(3):351–358
15. Markovic M., B. O. Fowler and M. S. Tung 2004, Preparation and comprehensive characterization of a calcium hydroxyapatite reference material. *J. Res. Natl. Inst. Stand. Technol.*, 109: 553- 568
16. Matsunaga K. and A. Kuwabara, 2007, First-principles study of vacancy formation in hydroxyapatite, *Phys. Rev. B*, 75(18), article ID: 014102
17. Mustafa M. AG., N. AG. Mustafa and R. S. Rasheed, effect of calcium and cole vit d3 in ovo injection on hatchability, bone and blood biochemical development at posthatch, *Iraqi Journal of Agricultural Sciences*, 50(3):850-856
18. Nafawaah S.M., 2017, Study of minerals that controlled calcium, magnesium and iron solubility and their relationships with soil conservation using solubility diagrams, *The Iraqi Journal of Agricultural Sciences*, 48(1): 0201-0271
19. Negrila C. C., M. V. Predoi, S. L. Iconaru and D. Predoi, 2018, Development of Zinc-Doped Hydroxyapatite by Sol-Gel Method for Medical Applications, *Molecules*, 23, 2986
20. Ofudje E. A., A. I. Adeogun, M. A. Idowu, and S. O. Kareem, 2019, Synthesis and characterization of Zn-Doped hydroxyapatite: scaffold application, antibacterial and bioactivity studies., *Heliyon*, 5(5): e01716
21. Phatai P., C. M. Futralan, S. Utara, P. Khemthong and Kamonwannasit, 2018, Structural characterization of cerium-doped hydroxyapatite nanoparticles synthesized by an ultrasonic-assisted sol-gel technique, *Results Phys.*, 10: 956-963
22. Predoi D., S. L. Iconaru, A. Deniaud, M. Chevallet, L. Michaud-Soret, N. Buton and et la., Textural, 2017, Structural and Biological Evaluation of Hydroxyapatite Doped with Zinc at Low Concentrations, *Materials*, 10, 229; doi:10.3390/ma10030229
23. Robert-Aguila M. J., J. A. Reyes-Avenidaño and M. E. Mendoza, 2017, Structural analysis of metal-doped (Mn, Fe, Co, Ni, Cu, Zn) calcium hydroxyapatite synthesized by a sol-gel microwave-assisted method, *Ceram. Int.*, 43 (15): 12705-12709
24. Stanić V., S. Dimitrijević, A. J. Stanković, M. Mitrić, B. Joki, I. B. Plečaš and S. Raičević 2010, Synthesis, characterization and antimicrobial activity of copper and zinc-doped hydroxyapatite nanopowders, *Appl. Surf. Sci.*, 256(20): 6083–6089
25. Zakian C., I. Pretty, R. Ellwood, 2009, Near-infrared hyperspectral imaging of teeth for dental caries detection, *J. Biomed. Opt.* 14 (6): 64047
26. Zhang D., H. Zhang, J. Wen, J. Cao, 2019, Preparation and characteristics of zinc and strontium co-doped hydroxyapatite whiskers, *IOP Conf. Ser.: Earth Environ. Sci.*, 233 022007
27. Zilm M. E., L. Chen, V. Sharma, A. Mc Dannald, M. Jain, R. Ramprasad and M. Wei, 2016, Hydroxyapatite substituted by transition metals: experiment and theory, *Phys. Chem. Chem. Phys.*, 18, 16457-164